

# Effect of Gravity on Liquid Plug Transport Through an Airway Bifurcation Model

Y. Zheng  
J. C. Anderson  
V. Suresh  
J. B. Grotberg

Phone: (734) 936-3834  
Fax: (734) 936-1905  
e-mail: grotberg@umich.edu

Department of Biomedical Engineering,  
University of Michigan, Ann Arbor, MI 48109

Many medical therapies require liquid plugs to be instilled into and delivered throughout the pulmonary airways. Improving these treatments requires a better understanding of how liquid distributes throughout these airways. In this study, gravitational and surface mechanisms determining the distribution of instilled liquids are examined experimentally using a bench-top model of a symmetrically bifurcating airway. A liquid plug was instilled into the parent tube and driven through the bifurcation by a syringe pump. The effect of gravity was adjusted by changing the roll angle ( $\phi$ ) and pitch angle ( $\gamma$ ) of the bifurcation ( $\phi = \gamma = 0$  deg was isogravitational).  $\phi$  determines the relative gravitational orientation of the two daughter tubes: when  $\phi \neq 0$  deg, one daughter tube was lower (gravitationally favored) compared to the other.  $\gamma$  determines the component of gravity acting along the axial direction of the parent tube: when  $\gamma \neq 0$  deg, a nonzero component of gravity acts along the axial direction of the parent tube. A splitting ratio  $R_s$  is defined as the ratio of the liquid volume in the upper daughter to the lower just after plug splitting. We measured the splitting ratio,  $R_s$ , as a function of: the parent-tube capillary number ( $Ca_p$ ); the Bond number ( $Bo$ );  $\phi$ ;  $\gamma$ ; and the presence of pre-existing plugs initially blocking either daughter tube. A critical capillary number ( $Ca_c$ ) was found to exist below which no liquid entered the upper daughter ( $R_s = 0$ ), and above which  $R_s$  increased and leveled off with  $Ca_p$ .  $Ca_c$  increased while  $R_s$  decreased with increasing  $\phi$ ,  $\gamma$ , and  $Bo$  for blocked and unblocked cases at a given  $Ca_p > Ca_c$ . Compared to the nonblockage cases,  $R_s$  decreased (increased) at a given  $Ca_p$  while  $Ca_c$  increased (decreased) with an upper (lower) liquid blockage. More liquid entered the unblocked daughter with a blockage in one daughter tube, and this effect was larger with larger gravity effect. A simple theoretical model that predicts  $R_s$  and  $Ca_c$  is in qualitative agreement with the experiments over a wide range of parameters. [DOI: 10.1115/1.1992529]

## Introduction

The propagation of liquid plugs or bubbles in channels and tubes has been studied for many applications from oil recovery from porous rock to medical treatments in the lung. Liquid plugs are instilled and transported through pulmonary airways in medical treatments such as surfactant replacement therapy (SRT) [1–5], partial liquid ventilation [6–10], and drug delivery [11–15]. The effectiveness of these treatments depends on liquid distribution in the lung and delivery to targeted regions through the branching airway network. When the liquid forms air-blown plugs, delivery and distribution depend on how the plugs split at airway bifurcations. Liquid distribution in the lung is affected by a number of factors including physical properties of the liquid (viscosity, density, surface tension at the air-liquid interface), gravitational orientation [16,17], airway geometry, instillation method [18,19], plug size [20], propagation speed [21], surface activity due to surfactants [22], and presence of other plugs in nearby airways [23] from previous instillations. It is therefore important to understand the effect of these factors on the basic process of plug splitting at airway bifurcations, which ultimately determines the final liquid distribution.

Previous studies have used animal models, benchtop experiments and theoretical models to study the effect of plug instillation methods and propagation speeds on liquid distribution in airways. Cassidy et al. [19] and Espinosa et al. [18] found that the formation of an initial liquid plug in the trachea followed by air

inspiration resulted in a more uniform distribution than the gravitational drainage of instilled liquid through the upper airways. Anderson et al. [21] investigated the effect of ventilation rate (i.e., propagation speed) on liquid distribution in excised rat lungs. They found that the liquid was delivered vertically more homogeneously at high ventilation rate compared to the low ventilation rate. Bull et al. [17] found that faster instillation rates of PFC into intact rabbit tracheas results in liquid plugs forming in large airways and more uniform distribution in rabbit lungs.

Cassidy et al. [23] performed experiments in glass capillaries and a benchtop model of an airway symmetric bifurcation in an iso-gravitational orientation to study plug dynamics and the effect of secondary plugs in daughter airways on plug splitting. They found that plug split evenly over the range of capillary numbers and plug volumes studied. When a secondary liquid plug was introduced as a blockage into one of the daughter tubes, more liquid entered the unblocked daughter. This effect was more pronounced at lower speeds (small  $Ca$ ) and larger blockage volumes.

The previous benchtop studies were conducted when gravity acted normal to the direction of motion and did not affect splitting at the bifurcation. However, studies have shown that gravity plays an important role in determining liquid distribution in the lung [17]. It was compared to the liquid distribution in intact rabbit lungs in the supine and upright positions at three constant infusion rates of perfluorocarbon (PFC). It was found that the supine posture resulted in more homogeneous filling of the lungs than the upright posture, in which liquid predominantly filled the inferior (gravitationally favored) regions of the lungs first. Ueda et al. [16] evaluated the effect of treatment technique, with different postures and different amounts of boluses, on surfactant distribution. They found that the surfactant distributions were similar for the bolus

Contributed by the Bioengineering Division for publication in the JOURNAL OF BIOMECHANICAL ENGINEERING. Manuscript received December 17, 2004. Final manuscript received April 20, 2005. Associate Editor: C. Ross Ethier.

treatment techniques but the infusion treatment resulted in very poor distribution which is assumed as the effect of maturation and gravity. These effects are due to the three-dimensional nature of the pulmonary airway network [24–26], in which different airways have different orientations with respect to gravity.

When a plug forms by the instilled liquid in pulmonary airways and reaches an airway bifurcation, the volume of liquid delivered to each branch may depend on gravity: more liquid enters the gravity-favored branch compared to the gravity-opposed one. This is repeated at each bifurcation and affects the overall distribution in the lung. Thus plug splitting at a single bifurcation is a basic feature of liquid transport in airways and our aim in this paper is to develop a better understanding of this process by means of experimental and theoretical studies of plug splitting in a benchtop model of an airway bifurcation. Experiments were performed in a benchtop model of an airway bifurcation that was oriented at different angles with respect to gravity. In some experiments a liquid plug was introduced in one of the daughter tubes to simulate the effect of a liquid plug in a downstream airway. A theoretical model of plug transport through an airway bifurcation was developed to predict the splitting ratio as a function of fluid properties, tube geometry, imposed flow rate and gravity and compared with the experimental results.

Dry tubes were used in our experiments whereas the walls of real airways are lined with a thin liquid layer. As a plug moves through the tube, it deposits a trailing liquid film in the rear. However, a moving solid-liquid-air contact line is present where the front meniscus meets the tube wall. This moving contact line requires additional forces (explained later) acting on the plug that are not exactly representative of real airways. Hence the use of dry tubes needs to be justified. From a practical standpoint, it is more difficult to do experiments with prewetted tubes lined with a precursor liquid film [23] since the liquid lining is unstable: hydrodynamic instabilities cause waves on the film surface to amplify [27,28] and form liquid plugs for thick films [29] or undulate collars in the tubes [30] for thin films. While such instabilities are relevant for airway closure [31–33], the focus of this study is the effect of gravity on plug splitting. The gravity was assumed to have no effect on the equilibrium contact angle [34]. In this study, as the meniscus speed is small, we expect that the comparisons between different orientations depend on gravity, not on the contact line forces. However, the contact line force is a physical force present in our experiments and its magnitude can be as large as the viscous force at low velocities, so we included this force in the theoretical analysis.

## Experimental Methods

**Experimental Setup.** Experiments were performed using a bench top model of a physiologic realistic airway bifurcation previously described by [23]. The diameter of the parent tube is 0.40 cm (5/32 inch) while that of each daughter tube is 0.32 cm (1/8 in.). The branch angle between two daughter tubes is 60 deg. The total cross-sectional area increases by 28% from the parent to the daughters. The airway dimensions and area increase accurately represent generations 5–7 in the adult human lung [24]. A detailed description of the bifurcation plate geometry and specifications can be found in [35] based on [36].

The flat inner surfaces of the bifurcation plates were coated with a thin layer of silicone rubber, clamped together and cured for 24 h to form an airtight seal. The plates were then fixed to a platform that could be oriented at different angles with respect to gravity by changing the roll angle  $\phi$  and the pitch angle  $\gamma$  as shown in Fig. 1. When  $\phi = \gamma = 0$ , gravity acts normal to the plane of the bifurcation plates and the system is isogravitational. When  $\phi > 0$ , the daughter tubes are asymmetrically oriented with respect to gravity, with daughter A being at a lower level than daughter B. Thus when a plug splits, more liquid tends to enter A compared to B. When  $\gamma > 0$  deg the plates are tilted so that gravity acts axially

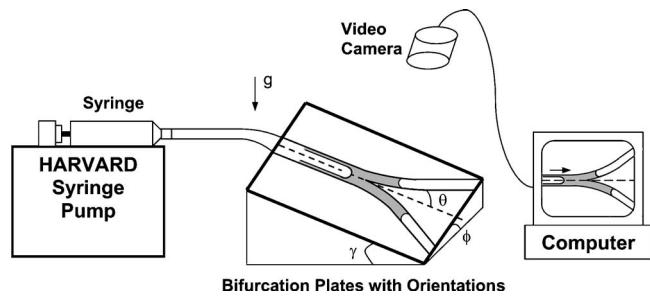


**Fig. 1 Schematic of the experimental setup. The roll angle,  $\phi$ , and pitch angle,  $\gamma$  describe the orientation of the bifurcation plates with respect to gravity. The branch angle of the daughter tube with respect to the parent tube is indicated by  $\theta$ .**

along the direction of liquid motion in the parent tube, whereas when  $\gamma < 0$  deg gravity acts against liquid motion through the parent. The airway model was connected to a positive displacement pump by flexible tubes and placed under a video camera (Veo Velocity Connect web camera), which is fixed perpendicular to the test section and connected to a computer. A plug of liquid was injected into the parent tube using a syringe and pumped through the bifurcation into the daughter tubes using a Harvard syringe pump with air as the driving fluid. Two different liquids, LB-400-X lubricant oil (Union Carbide Chemical) and glycerin were used as plug fluids. The speed of propagation was controlled by specifying the flow rate at the pump. Plug motion was recorded by the video camera at 30 frames/s and saved to the computer for further analysis. The experiment was repeated five times for each speed and orientation. After each run the system was flushed first with isopropyl alcohol and then deionized distilled water to remove plug fluid deposited on the channel walls. This process was repeated three to five times and the plates were finally flushed with isopropyl alcohol and then dried by blowing dry air at 20–25 psi for 2 min. The silicone rubber gasket was replaced once a week or when the plug fluid was changed. Two sets of experiments were performed to examine the effect of gravity on plug splitting. In the first case, experiments were performed at different roll and pitch angles ( $\phi = 15$  deg, 30 deg, 60 deg;  $\gamma = -15$  deg, 0 deg, 15 deg, 30 deg). A snapshot after plug splitting in such an experiment is shown in Fig. 2(a). In the second case, a second liquid plug was introduced as a blockage into one of the daughter tubes and plug splitting was studied for  $\phi = 15$  deg, 30 deg, 60 deg and  $\gamma = 0$  deg. A snapshot of such an experiment prior to plug splitting with daughter B blocked is shown in Fig. 2(b). The scale in the figures is in centimeters.

For each experiment, the saved images were analyzed to measure the lengths  $L_A$  and  $L_B$  Fig. 2(a) as the distance between two meniscus tips of the plugs in the daughter tubes immediately after the rear meniscus of the parent plug passed the carina and separated into two menisci. The propagation speeds of the rear meniscus of parent plug were measured from the recorded plug motion, from which the rear meniscus capillary number  $Ca_p = \mu U_p / \sigma$  was obtained ( $\mu$  and  $\sigma$  are viscosity and surface tension of plug fluid,  $U_p$  is rear meniscus speed of the parent plug). A splitting ratio  $R_s$  was defined as the ratio of liquid volume in daughter B to that in daughter A immediately after the parent plug splits into two. Since the diameters of two daughter tubes are equal,  $R_s = L_B / L_A$ . Mean values and standard errors for  $R_s$  and  $Ca_p$  were calculated from the five runs for each speed and orientation. To minimize the effect of plug size variation on the results, the parent plug length was measured just before it entered the expanding region of the parent tube and only cases where the plug length was  $1.5 \pm 0.1$  cm were considered.

**Parameter Definitions.** The relevant parameters include the physical properties of the liquids (viscosity  $\mu$ , density  $\rho$ , and air-

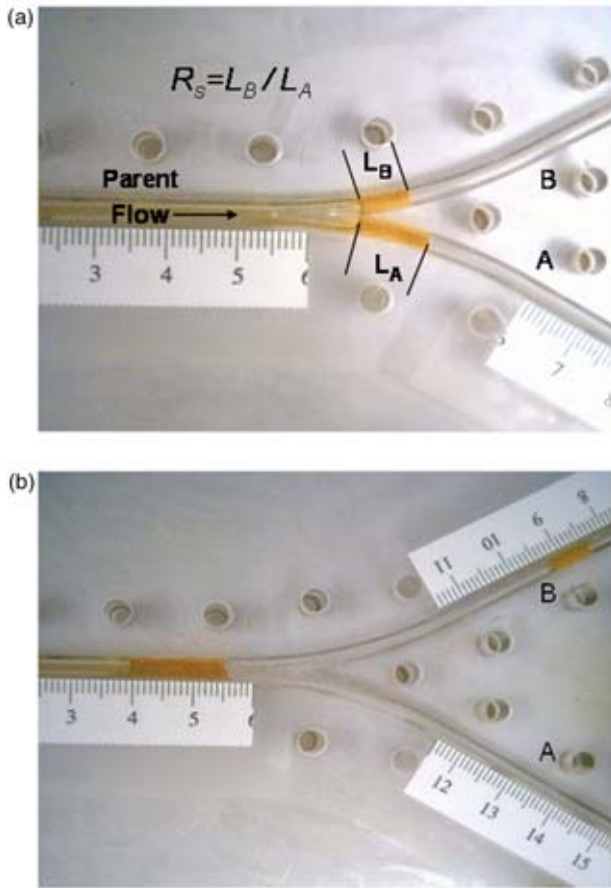


**Fig. 2** (a) An image of the plug immediately after it has entered two daughter branches and split. (b) Image of an experiment with blockage in daughter A.

liquid surface tension  $\sigma$ ), parent plug velocity ( $U_p$ ), the parent plug volume ( $V_p^*$ ), gravitational acceleration ( $g$ ), roll and pitch angles ( $\phi, \gamma$ ), branch angle  $\theta$ , contact angle at the front interfaces  $\alpha$ , parent tube radius ( $a_1$ ) and the daughter tube radius ( $a_2$ ). We choose to use the speed of the rear meniscus in the parent tube to characterize the plug speed, since it can be easily measured from the recorded images. For the blocked tube experiments, the volume of the blockage  $V_b$  is another parameter. These parameters are combined to obtain the following nondimensional groups: Capillary number  $Ca_p = \mu U_p / \sigma$ , Bond number  $Bo = \rho g a_1^2 / \sigma$ , Reynolds number  $Re_p = \rho U_p a_1 / \mu$ , dimensionless plug volume  $V_p = V_p^* / a_1^3$ , dimensionless blockage volume  $V_b = V_b^* / a_1^3$ , the radius ratio  $a_2 / a_1$ , and angles  $\theta, \phi, \gamma$ , and  $\alpha$ .  $Ca_p$  and  $Bo$  represent the ratio of viscous and gravitational forces to surface tension force respectively, while  $Re_p$  represents the ratio of inertial to viscous forces. For the purposes of these experiments the most important parameters are  $Ca_p$  (controlled by changing  $U_p$ ),  $\phi, \gamma$ , and  $Bo$ . Inertia of the plug fluid can be neglected if  $Re_p$  is small, which is true for the liquids and small velocities used. Values of the various dimensional and dimensionless parameters are listed in Table 1. Clinically relevant values of  $Ca_p, Bo, Re_p$ , and  $V_p$  have been discussed by [23] and the parameter space explored here lies in that range.

## Experimental Results

**Effect of Changing  $\phi$ .** The pitch angle was fixed at  $\gamma=0$  deg and experiments were performed for three values of the roll angle,  $\phi=15$  deg, 30 deg, 60 deg, and a number of different speeds such that  $0.001 < Ca_p < 0.11$ . In Fig. 3 the symbols show the experi-

**Table 1** Values for the two liquids and experimental conditions studied

Property	LB-400-X	Glycerin
$\mu$ (g/cm/s)	1.51	9.6
$\rho$ (g/cm <sup>3</sup> )	0.989	1.26
$\sigma$ (dyn/cm)	30.7	63.4
$L_0$ (cm)	$1.5 \pm 0.1$	$1.5 \pm 0.1$
$L_{b0}$ (cm)	$0.7 \pm 0.1$	$0.7 \pm 0.1$
$V_p$	$23.6 \pm 1.6$	$23.6 \pm 1.6$
$V_b$	$7.1 \pm 1$	$7.1 \pm 1$
$Bo$	1.26	0.78
$Ca_p$	0.001–0.11	0.005–0.11
$Re_p$	0.0027–0.3	0.0008–0.024
$\alpha_0$ (polycarbonate)	6.4 (deg)	56.3 (deg)

mental results for the mean values of  $R_s$  plotted against  $Ca_p$  for different  $\phi$ . The bidirectional bars on each experimental point represent the standard error. In all cases a larger fraction of the plug liquid entered the lower daughter, A, than daughter, B, after bifurcation and so  $R_s < 1$ . Note that for each  $\phi$  there is a critical value of the capillary number,  $Ca_p = Ca_c$  below which  $R_s = 0$ , i.e., no liquid enters the upper daughter. Thus a minimum speed (pressure) is needed for the liquid to overcome gravity and enter the upper daughter after bifurcation. For  $Ca_p > Ca_c$ ,  $R_s$  increases with  $Ca_p$  and the slope of  $R_s$ - $Ca_p$  curve decreases. In contrast, results for the isogravitational case [23] ( $\phi = \gamma = 0$  deg) showed that  $R_s \approx 1$  for all  $Ca_p$  and did not indicate the existence of a critical capillary number. As  $\phi$  increases, Fig. 3 indicates that  $Ca_c$  increases and  $R_s$  decreases at a given  $Ca_p > Ca_c$ . These observations are consistent with the increasing gravitational asymmetry between the two daughters.

**Effect of Changing  $\gamma$ .** Experiments were performed for four values of the pitch angle  $\gamma = -15$  deg, 0 deg, 15 deg, 30 deg with the roll angle fixed at  $\phi = 30$  deg and  $0.001 < Ca_p < 0.1$ . Experiments with  $\gamma \neq 0$  deg and  $\phi = 0$  deg were performed, and it is found that  $R_s = 1$  with  $\phi = 0$  deg. To study the effect of pitch angle, we studied the case with nonzero roll angle and let  $\phi = 30$  deg. Results are plotted in Fig. 4 with the symbols representing experimental results. When  $\gamma = -15$  deg,  $R_s > 0$  for all  $Ca_p$  chosen. Critical capillary numbers  $Ca_c$ , that increase with  $\gamma$ , were found for

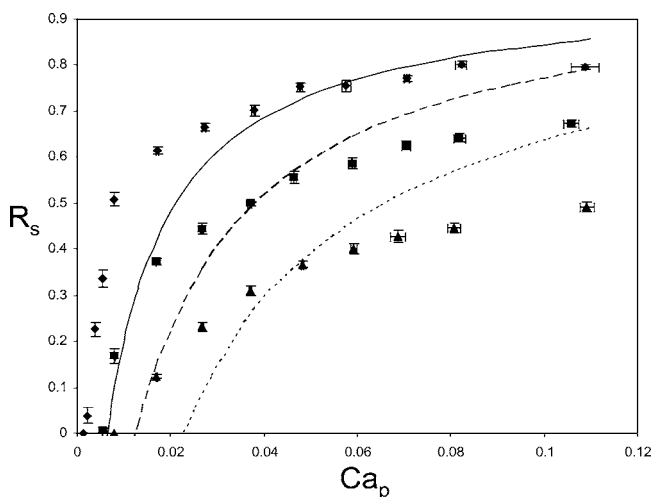


**Fig. 3**  $R_s$  vs  $Ca_p$  for  $\gamma=0$  deg and different  $\phi$  using LB-400-X oil.  $\phi=15$  deg:  $\blacklozenge$  (experiments), — (theory);  $\phi=30$  deg:  $\blacksquare$  (experiments), --- (theory);  $\phi=60$  deg:  $\blacktriangle$  (experiments), ... (theory).

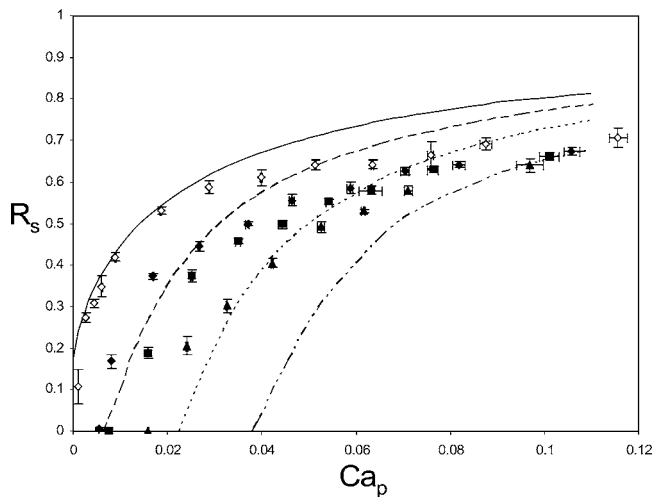


**Fig. 4**  $R_s$  vs  $Ca_p$  for  $\phi=30$  deg and different  $\gamma$  using LB-400-X oil.  $\gamma=-15$  deg:  $\diamond$  (experiments), — (theory);  $\gamma=0$  deg:  $\blacklozenge$  (experiments), - - - (theory);  $\gamma=15$  deg:  $\blacksquare$  (experiments),  $\cdots$  (theory);  $\gamma=30$  deg:  $\blacktriangle$  (experiments), — (theory).

$\gamma > 0$  deg.  $R_s$  decreases with  $\gamma$  for a given  $Ca_p > Ca_c$ . However, when  $Ca_p > 0.1$ ,  $R_s$  seems to asymptote to a value  $\sim 0.7$  independent of  $\gamma$ . These results indicate that the effect of gravity in axial direction is more important at low speeds than high speeds. At low speeds, the flow contribution to the pressure drop  $P_1 - P_a$  is small and the hydrostatic pressure due to axial gravity dominates. Since this component varies with  $\gamma$ ,  $R_s$  is a function of  $\gamma$  at small  $Ca_p$ . At high speeds, the flow contribution dominates the pressure drop and thus changing  $\gamma$  has only a small effect on  $R_s$ . For  $\gamma > 30$  deg or  $\gamma \leq -30$  deg it was not possible to form a stable plug in the parent tube and the liquid drained as a film along the bottom of the parent tube.

**Effect of Blockages in the Daughter Tubes.** Experiments were performed with a liquid plug introduced as a blockage into one of the daughter tubes and  $Ca_p$  and  $R_s$  were measured. Experiments were performed separately for blockages in the upper and lower daughters. The length of the blockages is shown in Table 1. Experimental results are plotted as symbols shown in Fig. 5(a)–5(c) for the orientations  $\phi=15$  deg, 30 deg, 60 deg;  $\gamma=0$  deg. Data from the unblocked experiments of Fig. 3 are included for comparison. In the unblocked case, more liquid enters the lower daughter which is gravity preferred. The presence of a blockage in one of the daughter tubes introduces an additional asymmetry, which can counteract or enhance the gravitational asymmetry. The figures show that a blockage in the lower daughter tends to oppose the effect of gravity and results in larger  $R_s$ . In fact, this effect can overcome gravity and cause more liquid to enter the upper daughter than the lower daughter, leading to  $R_s$  values as high as 1.26 in Fig. 5(a) ( $\phi=15$  deg). The same effect is seen in Fig. 5(b) and 5(c) for the larger roll angles ( $\phi=30$  deg, 60 deg), but  $R_s$  values are smaller due to the greater effect of gravity in these more asymmetric orientations. In contrast blockages in the upper daughter accentuate the gravitational asymmetry and lead to smaller values of  $R_s$  compared to the unblocked case. These results are consistent with [23] who found that more liquid tends to enter the unblocked daughter in the isogravitational case. The effect of the blockages can be quite significant. A blockage in the lower daughter reduces  $Ca_c$  and at  $Ca_p < 0.03$ , a blockage in the lower daughter can increase  $R_s$  by 200% to 1000% while at  $Ca_p > 0.03$ ,  $R_s$  increases by 50%–100% compared to the unblocked Fig. 5(a)–5(c). In contrast, a blockage in the upper daughter increases  $Ca_c$  and  $R_s$  can decrease by 40%–80% at  $Ca_p > 0.02$  while

by 200%–600% at  $Ca_p < 0.02$ . These effect become more noticeable as  $\phi$  is increased from 15 deg to 60 deg. Another interesting observation is the presence of maxima in the  $R_s$ - $Ca_p$  curves in [5(a) and 5(b)] when the lower daughter is blocked. The maximum is most noticeable at the smaller roll angle,  $\phi=15$  deg Fig. 5(a) but disappears when  $\phi=60$  deg Fig. 5(c). In some clinical study, a pretreatment as a blockage in nearby airway branches can be introduced, which may be effective to control the liquid delivery to a targeted position in the lung.

**Effect of Bo.** Two different liquids, LB-400-X oil ( $Bo=1.26$ ) and glycerin ( $Bo=0.78$ ), were used to study the effect of changing  $Bo$  on  $R_s$  at  $\phi=60$  deg,  $\gamma=0$  deg. The static contact angle of LB-400X oil on polycarbonate plate is measured about 6.4 deg using a video camera, consistent with [37] in which the static contact angle of silicone oil, with similar physical properties as LB-400X, on polycarbonate plate is 6.2 deg. The static contact angle of glycerin on polycarbonate plate is measured as 56.3 deg. We expect that the difference in  $R_s$  is mainly due to the difference in  $Bo$  not the variation of static contact angle  $\alpha_0$  since it is predicted in the next section “Theoretical Analysis” that  $R_s$  varies within 5% when only changing static contact angle  $\alpha_0$  from 0 deg to 60 deg. Results are plotted as symbols in Fig. 6 and indicate that a 60% change in  $Bo$  leads to a 10%–50% change in  $R_s$  for  $0.007 < Ca_p < 0.14$ .  $R_s$  is more sensitive to  $Bo$  at lower  $Ca_p$  which is because at low speeds gravity contribution to pressure drop is more important, therefore changing  $Bo$  leads to bigger changes in  $R_s$ .

## Theoretical Analysis

To better understand the fluid transport of plug splitting process, a theoretical model was developed to predict or compare the experimental results. A schematic model of plug splitting with all the dimensions is shown in Fig. 7. For simplification, the curved tubes of the experimental bifurcation model are replaced by straight tubes. The branch angle in the experiments is a function of the distance from the bifurcation, since the proximal segments of the daughter tubes have a nonzero axial curvature. The initial value of the branch angle at the bifurcation is  $\theta=10$  deg and the distal value starting at approximately 3 cm from the bifurcation is  $\theta=30$  deg. For the theory we selected a constant average value,  $\lambda=20$  deg. The plug lengths were shorter than 3 cm, so this seems a reasonable approximation. The motion of the plug is considered to be quasi-steady and expressions for the splitting ratio  $R_s$  are derived by a theoretical calculation of the pressure drops and mass balances between the parent and daughter tubes. The effect of gravity on the meniscus shape of the air-liquid interface, which has been studied in Suresh and Grotberg [38] is neglected. The pressure drop between the parent and daughter tubes has different contributions. It includes the capillary jump across the air-liquid interfaces, viscous resistance estimated with Poiseuille’s Law, gravitational hydrostatic effects and the effect of moving contact lines at the air-liquid interface in the daughter tubes. Each of these is discussed separately below.

First, consider the mass balance. The flow rate in the parent tube must be equal to the sum of flow rates in the daughters, i.e.,

$$Q_1 = Q_2 + Q_3, \quad (1)$$

where  $Q_i = \pi a_i^2 U_i$  is the flow rate in the parent tube ( $i=1$ ) and daughter tubes ( $i=2, 3$ ) with  $a_i$  and  $U_i$  being the radius and mean front meniscus speed.  $U_1$  is the speed of the front meniscus of the plug in the parent tube. It can only be defined until the meniscus enters the daughter tubes at the beginning of splitting. Later in the section we will relate  $U_1$  to the rear meniscus speed  $U_p$  in the parent tube which can be defined until plug splitting is complete. Since the plug motion is assumed to be quasisteady and  $a_2=a_3$ , the splitting ratio is given by

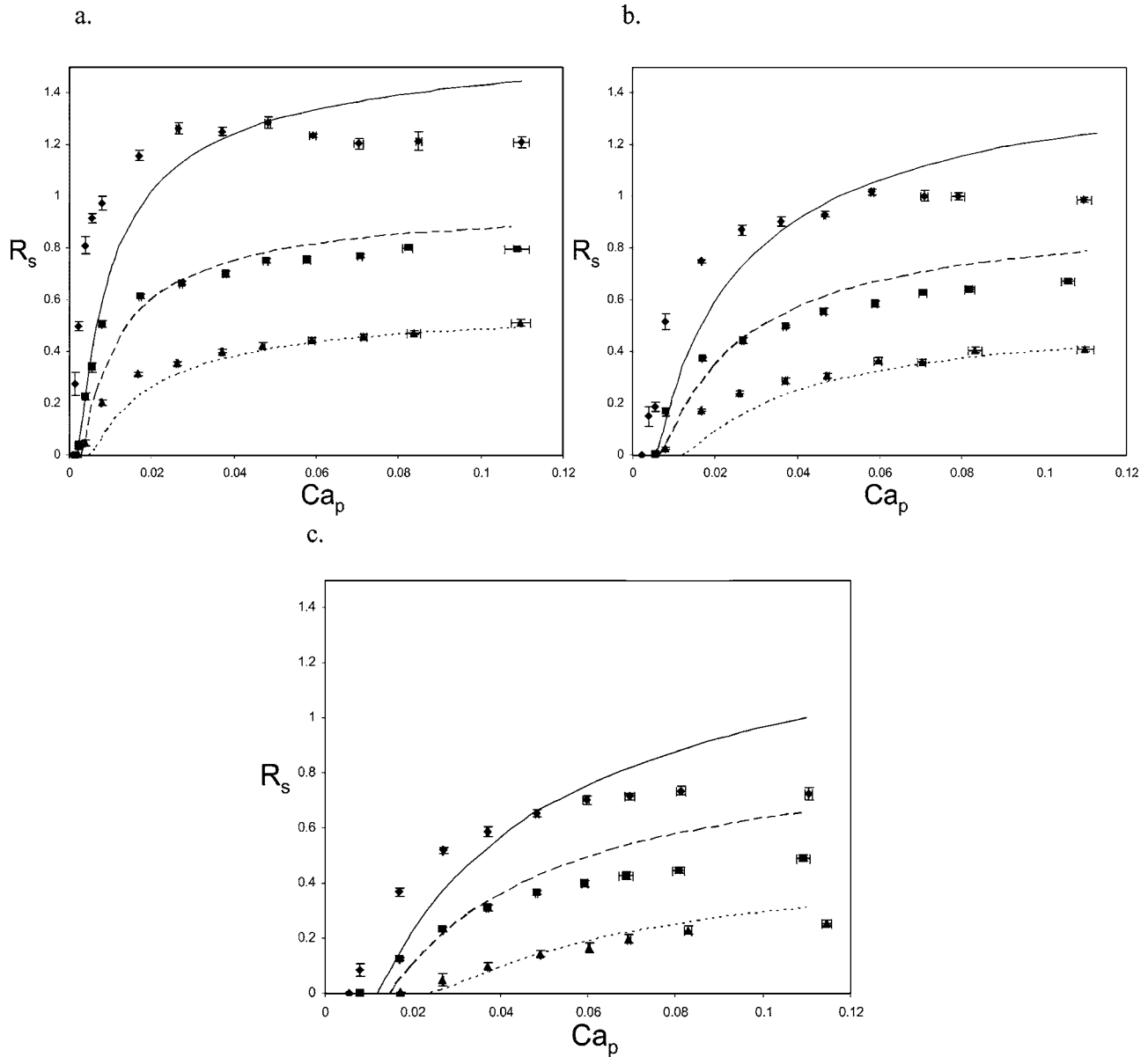


Fig. 5  $R_s$  vs  $Ca_p$  for  $\gamma=0$  deg and different blockage conditions using LB-400-X oil with a pitch angle  $\gamma=0$  deg and a roll angle of  $\phi=15$  deg (panel a),  $\phi=30$  deg (panel b), and  $\phi=60$  deg (panel c). Blockage in lower daughter:  $\blacklozenge$  (experiment), — (theory); No blockage:  $\blacksquare$  (experiment), --- (theory); Blockage in upper daughter:  $\blacktriangle$  (experiment),  $\cdots$  (theory).

$$R_s = Q_2/Q_3 = U_2/U_3 = L_2/L_3, \quad (2)$$

where  $L_2$  and  $L_3$  are the lengths of the liquid plug in the daughter tubes at any time. From (1) and (2) the flow rates and capillary numbers in the daughter tubes can be related to those in the parent tube as

$$Q_2 = \frac{R_s}{R_s + 1} Q_1, \quad Q_3 = \frac{1}{R_s + 1} Q_1; \quad (3)$$

$$Ca_2 = \left(\frac{a_1}{a_2}\right)^2 \frac{R_s}{R_s + 1} Ca_1, \quad Ca_3 = \left(\frac{a_1}{a_2}\right)^2 \frac{1}{R_s + 1} Ca_1 \quad (4)$$

Suppose  $L_0$  is the plug length in the parent tube just as the front meniscus reaches the bifurcation. As the plug moves towards the daughters, it deposits a trailing film of thickness  $h$  in the parent tube. Let the plug length in the parent tube be  $L_1 < L_0$  when the plug has partially entered the daughter tubes, as shown in Fig. 7.

Conservation of liquid mass requires the following relationship to be satisfied:

$$\pi a_1^2 L_0 - (\pi a_1^2 - \pi(a_1 - h)^2)(L_0 - L_1) = \pi a_2^2 (L_2 + L_3) \quad (5)$$

From (2) and (5) we then obtain

$$L_3 = \left(\frac{a_1}{a_2}\right)^2 \frac{L_0 - \left(1 - \left(1 - \frac{h}{a_1}\right)^2\right)(L_0 - L_1)}{R_s + 1} \quad (6)$$

Numerical studies by [39] showed that, when liquid inertia and gravity are neglected,  $h$  depends on the speed of propagation and the tube radius according to the relation

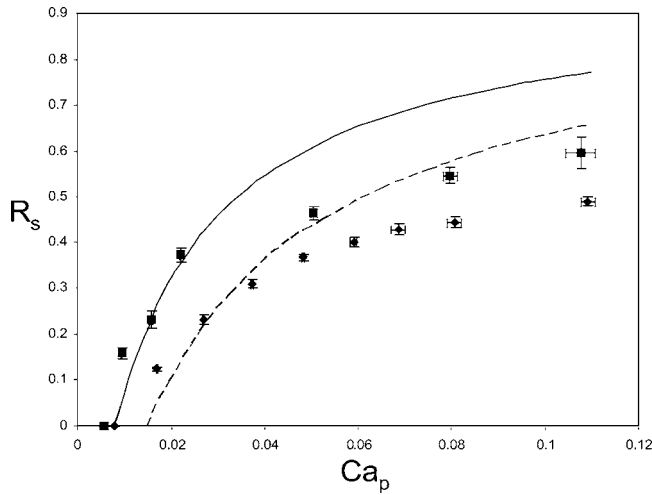


**Fig. 6**  $R_s$  vs  $Ca_p$  at  $\phi=60$  deg,  $\gamma=0$  deg for different Bo. Glycerin Bo=0.78: ■ (experiments), — (theory); LB-400-X Bo=1.26: ◆ (experiments), --- (theory).

$$\frac{h}{a_1} = 0.36(1 - e^{-2Ca_p^{0.523}}), \quad (7)$$

where  $Ca_p$  is a capillary number based on the speed  $U_p$  of the rear meniscus. We use (7) as an approximate expression for the trailing film thickness in our theoretical model. The neglect of liquid inertia is justified at the small speeds of the experiments, however (7) does not account for the variation of the trailing film thickness along the tube circumference due to gravitational effects.  $U_p$  is related to the mean front meniscus speed  $U_1$  by

$$Q_1 = \pi a_1^2 U_1 = \pi(a_1 - h)^2 U_p. \quad (8)$$

So

$$Ca_1 = \left(1 - \frac{h}{a_1}\right)^2 Ca_p. \quad (9)$$

Now consider the pressure drop between the parent and daughter tubes. In the parent tube, the difference between the air pressure  $P_1$  and the liquid pressure  $\pi_1$  at the rear meniscus is equal to

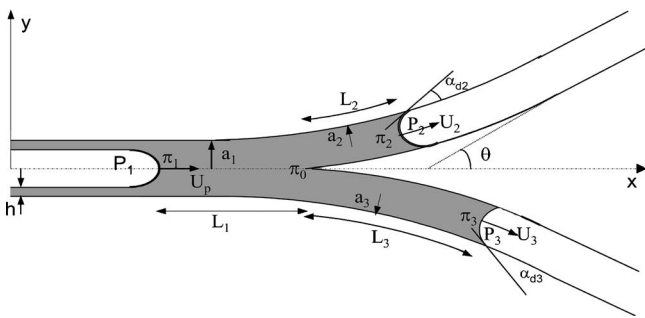


**Fig. 7** Schematic of plug flow in the bifurcation plates.  $a_1$ ,  $a_2$ , and  $a_3$  are the radius of the parent, upper and lower daughter tube respectively.  $P_1$  is the pressure of the pumped air.  $P_2$  and  $P_3$  are atmospheric pressure.  $L_1$ ,  $L_2$ , and  $L_3$  are the plug lengths in the parent, upper, and lower daughter tube, respectively.  $\pi_1$ ,  $\pi_0$ ,  $\pi_2$ , and  $\pi_3$  are the pressures in the liquid plug at the rear interface, bifurcation zone, front meniscus of upper daughter, and front meniscus of lower daughter, respectively.  $U_p$ ,  $U_2$ , and  $U_3$  are the plug velocities of rear meniscus in parent tube and front menisci in upper daughter and lower daughter tubes.

$$P_1 - \pi_1 = \frac{2\sigma}{a_1 - h}, \quad (10)$$

which represents the Young-Laplace Law for the capillary pressure jump across a *static* hemispherical interface whose radius  $r$  is equal to the tube radius minus the film thickness ( $r = a_1 - h$ ). Since the meniscus velocity is very small, the viscous effect is neglected for the pressure drop across the interface. The pressure drop within the plug liquid is approximated by the Poiseuille Law for flow in tubes. For long plug length and small capillary number, this assumption is valid and simplifies the calculations. We neglect the entrance effects and secondary flows that prevail when liquid enters the daughter tubes. We do not expect these features to have much effect on the splitting ratio since the inertia is negligible and capillary number is small. Also, a hydrostatic pressure drop resulting from gravity is included. Thus, in the parent tube

$$\pi_1 - \pi_0 = \frac{8\mu Q_1 L_1}{\pi a_1^4} - \rho g L_1 \sin \gamma. \quad (11)$$

Similarly, pressure drops can be written for the upper daughter [Eq. (12)] and lower daughter [Eq. (13)].

$$\pi_0 - \pi_2 = \frac{8\mu Q_2 L_2}{\pi a_2^4} + \rho g L_2 (\sin \theta \sin \phi - \cos \theta \sin \gamma) \quad (\text{B, upper}), \quad (12)$$

$$\pi_0 - \pi_3 = \frac{8\mu Q_3 L_3}{\pi a_3^4} - \rho g L_3 (\sin \theta \sin \phi + \cos \theta \sin \gamma) \quad (\text{A, lower}). \quad (13)$$

The capillary jumps at the air-liquid-solid interfaces in the daughter tubes are given by

$$\pi_2 - P_2 = -\frac{2\sigma}{a_2} \cos \alpha_{d2}, \quad (14)$$

$$\pi_3 - P_3 = -\frac{2\sigma}{a_3} \cos \alpha_{d3}, \quad (15)$$

where the dynamic contact angles  $\alpha_{d2}$  and  $\alpha_{d3}$  depend on the speed of the interfaces, and hence on the front meniscus capillary numbers,  $Ca_2$  and  $Ca_3$ . This dependence was modeled using an empirical correlation given by Bracke et al. [40]

$$\frac{\cos \alpha_d - \cos \alpha_0}{\cos \alpha_0 + 1} = -2 Ca^{1/2}, \quad (16)$$

where  $\alpha_0$  is the static contact angle at the three phases contact line. Equation (16) is an empirical equation which predicts the dependence of the dynamic contact angle on the static contact angle and the meniscus capillary number under air entrainment conditions. The equation was obtained from the experiments with a strip drawn into a large pool of liquid. We also tried one of the first empirical correlations given by Jiang [41], which is based on data published by Hoffman [42] from a study of non-polar liquids forced to spread through a glass capillary tube,

$$\frac{\cos \alpha_d - \cos \alpha_0}{\cos \alpha_0 + 1} = -\tanh(4.96 Ca^{0.702}). \quad (17)$$

The two correlations give results which are within 5%–10%. In our study, the capillary number covers from  $10^{-3}$  to  $10^{-1}$ . Bracke et al. [40] gave a relatively simple correlation and matches the range of capillary number we investigated.

When there is no blockage in the daughter tubes, the difference in the air pressure between the parent and the two daughter tubes can be found by combining Eqs. (10)–(16) to be

$$P_1 - P_a = \frac{2\sigma}{a_1 - h} - \frac{2\sigma}{a_2} \cos \alpha_{d2} + \frac{8\mu Q_1 L_1}{\pi a_1^4} - \rho g L_1 \sin \gamma + \frac{8\mu Q_2 L_2}{\pi a_2^4} + \rho g L_2 (\sin \theta \sin \phi - \cos \theta \sin \gamma) \quad (18)$$

$$P_1 - P_a = \frac{2\sigma}{a_1 - h} - \frac{2\sigma}{a_3} \cos \alpha_{d3} + \frac{8\mu Q_1 L_1}{\pi a_1^4} - \rho g L_1 \sin \gamma + \frac{8\mu Q_3 L_3}{\pi a_3^4} - \rho g L_3 (\sin \theta \sin \phi + \cos \theta \sin \gamma) \quad (19)$$

Equating (18) and (19), using (1)–(9), an equation relating  $R_s$  and the other parameters is obtained:

$$\begin{aligned} & 8 \left( \frac{a_1}{a_2} \right)^4 \text{Ca}_p \left( 1 - \frac{h}{a_1} \right)^2 (R_s - 1) + \text{Bo} (R_s + 1) \sin \theta \sin \phi \\ & - \text{Bo} (R_s - 1) \cos \theta \sin \gamma \\ & + 4 \left( \frac{a_1}{a_2} \right)^2 \frac{\left[ \text{Ca}_p \left( 1 - \frac{h}{a_1} \right)^2 \right]^{1/2} (\cos \alpha_0 + 1)}{(L_3/a_1)} \frac{(R_s^{1/2} - 1)}{(R_s + 1)^{1/2}} = 0 \end{aligned} \quad (20)$$

Equation (20) is solved numerically to determine  $R_s$  for given flow rate ( $\text{Ca}_p$ ), orientation ( $\phi, \gamma$ ), Bo and plug length ( $L_0$ ). The first term in Eq. (20) represents the flow (viscous) effects, the second and third terms represent the gravity effect and the last term expresses the moving contact line effects at the front menisci. All the theoretical curves for LB-400X are plotted with the static contact angle  $\alpha_0$  fixed at 6.4 deg, while for glycerin,  $\alpha_0 = 56.3$  deg.

When a plug is introduced into one of the daughter tubes as a blockage, there is an additional pressure drop in that daughter: viscous drag within the blockage and capillary jump across two menisci of the plug blockage including the new trailing film of the moving blockage. We assume that the blockage remains stationary until the parent plug begins to split and then moves at the same speed as the liquid entering that branch. While in the experiments, it was observed that the blockages start moving before the plug starts to split, which may contribute for the discrepancy of the theory and experiments. If the length of the blockage at any time is  $L_b$  and its flow rate is  $Q_b$ , the pressure drop across it is equal to

$$\begin{aligned} \Delta P_{\text{BLK}} &= \frac{2\sigma}{a_2 - h_2} - \frac{2\sigma}{a_2} \cos \alpha_d + \frac{8\mu Q_b L_b}{\pi a_2^4} \pm \rho g L_b \sin \theta \sin \phi \\ & - \rho g L_b \cos \theta \sin \gamma, \end{aligned} \quad (21)$$

where the positive and negative signs in  $\pm$  refer to the upper and lower daughters, respectively. Since the blockage moves the same distance as the length of the bifurcating plug entering that daughter, conservation of mass requires that  $L_b$  and the known initial blockage length  $L_{b0}$  are related as

$$\pi a_i^2 L_b = \pi a_i^2 L_{b0} - \pi (a_i^2 - (a_i - h_i)^2) L_i, \quad (22)$$

where  $i=2$  if the blockage is in the upper daughter and  $i=3$  if it is in the lower daughter. The trailing film thickness  $h_i$  is related to the local capillary number by (7). The pressure drop in Eqs. (18) or (19) is modified by adding this contribution and the following equations are obtained for blockages in the lower and upper daughters respectively:

$$\begin{aligned} & 8 \left( \frac{a_1}{a_2} \right)^4 \text{Ca}_p \left( 1 - \frac{h}{a_1} \right)^2 \left( (R_s - 1) - \frac{L_b}{L_3} \frac{1}{R_s + 1} \right) + \text{Bo} \left( R_s + 1 \right. \\ & \left. + \frac{L_b}{L_3} \right) \sin \theta \sin \phi - \text{Bo} \left( R_s - 1 - \frac{L_b}{L_3} \right) \cos \theta \sin \gamma - \frac{2a_1^2}{a_2 L_3} \\ & \times [(1 - \cos \alpha_0) - (1 + \cos \alpha_0)(2\text{Ca}_2^{1/2} - 4\text{Ca}_3^{1/2})] = 0 \end{aligned} \quad (23)$$

$$\begin{aligned} & 8 \left( \frac{a_1}{a_2} \right)^4 \text{Ca}_p \left( 1 - \frac{h}{a_1} \right)^2 \left( (R_s - 1) + \frac{L_b}{L_3} \frac{R_s}{R_s + 1} \right) + \text{Bo} \left( R_s + \frac{L_b}{L_3} \right. \\ & \left. + 1 \right) \sin \theta \sin \phi - \text{Bo} \left( R_s + \frac{L_b}{L_3} - 1 \right) \cos \theta \sin \gamma + \frac{2a_1^2}{a_2 L_3} \\ & \times [(1 - \cos \alpha_0) + (1 + \cos \alpha_0)(4\text{Ca}_2^{1/2} - 2\text{Ca}_3^{1/2})] = 0 \end{aligned} \quad (24)$$

Theoretical results for  $R_s$  in the presence of liquid blockages are obtained by numerically solving (23) (lower blockage) or (24) (upper blockage).

## Discussion

**Comparison of Theoretical and Experimental Results.** We used a simplified theoretical model, which qualitatively captures the features of the experimental data.

Fig. 3 and 4 shows how a comparison of the experimental data (symbols) with theoretical predictions for  $R_s$  (lines) for different  $\phi$  and  $\gamma$ . The theory captures the trends of the experimental data: (1) the existence of a critical capillary number, (2) the increase of  $R_s$  with  $\text{Ca}_p$  and its decreasing slope, and (3) the decrease of  $R_s$  with increasing  $\phi$ . When  $\gamma=0$  deg Fig. 3 shows that there is qualitative agreement between the theory and experiments, which is promising given the simplifying assumptions of the theory. The agreement is better for smaller values of  $\phi$ . At lower values of  $\text{Ca}_p$ , the theory underpredicts  $R_s$ , which leads to an overprediction of the critical capillary number. At higher values of  $\text{Ca}_p$ ,  $R_s$  is overpredicted. Fig. 4 shows  $R_s$  as a function of  $\text{Ca}_p$  for different values of  $\gamma$ . For  $\gamma=-15$  deg, the theory does not predict the existence of  $\text{Ca}_c$ , but agrees fairly well with experiments for  $\text{Ca}_p < 0.04$ . For other values of  $\gamma$ , the theory underpredicts  $R_s$  for small  $\text{Ca}_p$ , while for large  $\text{Ca}_p$ , the theory overpredicts  $R_s$  for all values of  $\gamma$ . The discrepancy between the theory and experiments increases with  $\gamma$ .

Figures 5(a)–5(c) show comparisons of theory and experiments with the effect of blockages. The theory is more accurate when the upper daughter is blocked and for smaller values of  $\phi$ . Also the theory is unable to predict the maxima in the experimental  $R_s$ - $\text{Ca}_p$  curve observed when the lower daughter is blocked.

Figure 6 compares theoretical and experimental results for different Bond numbers. It is seen that the theoretical results show bigger changes when Bo is varied than the experiments, but they agree qualitatively.

The discrepancies between theory and experiment are a result of approximations to the geometry of the model and the fluid dynamics in the theoretical analysis. The simplified theoretical model does not account for the transition in geometry from the bifurcating region of the parent tube to the daughter tubes. Pressure drops in the liquid were computed under the assumption of Poiseuille flow. While this assumption is accurate for a long plug in the parent tube [43], entrance and transient effects are likely to be important when the bifurcating plug enters the daughter tubes. The unsteady effect in the motion of the plug is neglected in the theory, which may play a complicated role in the experiments especially when the daughter blockages are present. It was observed in the experiments that the blockages start moving before the parent plug splits and plug speeds entering the daughter tubes are not constant so that the ratio  $L_A/L_B$  changes over the course of plug splitting.

**Experimental Limitations.** Although the present system allows us to evaluate the effect of gravity across a single bifurcation, it contains certain physiological limitations in its application to the pulmonary system. The physical dimensions of the model and flow rates used are relevant to plug propagation in the central airways (around generation 5–7), but not the trachea or larger airways. The bifurcation region in our model is a sharp corner instead of a rounded corner consistent to physiology, so the pressure drop across this region may be different with the real pulmonary airways. In our experiments, the plug is instilled manually

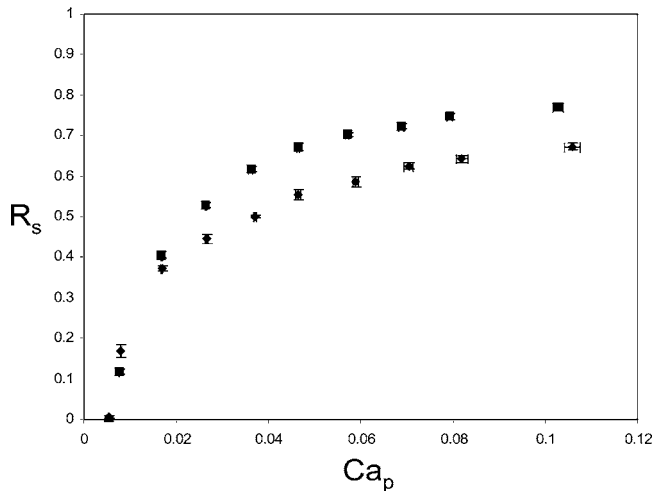


**Fig. 8** Experimental results of effect of parent plug volume on splitting ratio,  $R_s$ , and capillary number,  $Ca_p$  for LB-400-X oil at  $\phi=30$  deg,  $\gamma=0$  deg ■:  $L_0=3$  cm ( $L_0/a_1=15$ ), ◆:  $L_0=1.5$  cm ( $L_0/a_1=7.5$ ).

into the upstream region of the parent tube. The length of the parent plug is measured just before the leading meniscus enters the central zone of the bifurcation to get the parent plug volume. It is difficult to consistently deliver a parental plug of 1.5 cm in length, but care was taken to ensure that the length did not vary by more than 10% between experiments. For experiments with blocked daughter tubes, variations in the blockage plug lengths were also maintained to within 10%. Previous experiments have shown  $R_s$  depends weakly on the plug and blockage lengths [23]. In order to study the effect of plug length on  $R_s$ , we performed a set of experiments by doubling the parent plug length to 3 cm. Results are shown in Fig. 8. The critical capillary number was found to be unaffected by the plug length. For  $Ca_p < 0.01$ , doubling the plug length was found to decrease  $R_s$  by about 20%. For  $Ca_p > 0.01$ ,  $R_s$  for the longer plug was about 15% larger than the shorter plug. Since the variation in plug length in our experiments was small ( $L_0=1.5\pm 0.1$  cm), we do not expect significant effects on  $R_s$  from plug length effects. Larger Ca experiments in which the plugs entering the daughter branches are very short have a greater potential for error since small variations in measuring plug lengths can lead to large changes in  $R_s$ .

## Conclusion

We have used a combination of experiments and theory to study the effects of gravity and liquid blockages in downstream branches on liquid plug splitting in a bench top model of a physiologically realistic airway bifurcation. The experiments demonstrate a critical capillary number  $Ca_c$  below which the entire plug drains into the gravitationally favored daughter leading to a splitting ratio  $R_s=0$ . For capillary numbers greater than the critical value ( $Ca_p > Ca_c$ ),  $R_s$  depends on  $Ca_p$ , the roll angle  $\phi$  and pitch angle  $\gamma$ .  $R_s$  increases with  $Ca_p$  at a given  $\phi$  and  $\gamma$  while  $R_s$  decreases with increasing  $\phi$  and  $\gamma$  at a given  $Ca_p$ . As  $Ca_p$  increases  $R_s$  approaches a limiting value, which decreases with  $\phi$ , but seems to be independent of  $\gamma$ . Higher Bond numbers enhance the effect of gravity and lead to lower splitting ratios. This effect was more significant at low  $Ca_p$ , but less important at higher  $Ca_p$ . Experiments were also performed with a liquid blockage in one of the daughter tubes. The presence of a blockage in the lower, gravitationally favored daughter counteracts the effect of gravity and results in larger splitting ratios compared to the unblocked case. When the upper daughter is blocked gravitational asymmetry is enhanced which causes smaller values of  $R_s$ . A simplified theoret-

ical model that accounted for pressure drops across the tubes due to surface tension, gravity, viscosity, and moving contact line effects was developed. Predicted values of  $R_s$  capture the experimental trends and agree qualitatively with the data over a range of parameters.

This study provides some insights into the physical mechanisms that affect liquid plug transport in airways and quantifies the effects of flow rate, gravitational orientation and downstream liquid blockages. It represents a first step towards the development of a rational strategy to achieve targeted liquid delivery by manipulating ventilation (flow) rate, posture (gravitational orientation) and instillation methods that promote or deter liquid plug formation in distal airways. The parameter range studied in this work is applicable to central airways in which the fluid velocity is relatively low. Future studies will examine faster speeds and the role of liquid inertia which are important in larger airways.

## Acknowledgments

This work is supported by NIH Grant Nos. HL-41126, HL64373, NSF Grant No. BES-9820967, NASA Grant Nos. NAG3-2196 and NAG3-2740 The authors want to thank J. C. Grotberg for his technical support and Dr. Fujioka for his helpful discussions.

## References

- Long, W., Thompson, T., Sundell, H., Schumacher, R., Volberg, F., and Guthrie, R., 1991, "Effects of Two Rescue Doses of a Synthetic Surfactant on Mortality Rate and Survival Without Bronchopulmonary Dysplasia in 700- to 1350-gram Infants with Respiratory Distress Syndrome. The American Exosurf Neonatal Study Group I," *J. Pediatr.*, **118**, pp. 595-605.
- Corbet, A., Bucciarelli, R., Goldman, S., Mammel, M., Wold, D., and Long, W., 1991, "Decreased Mortality Rate Among Small Premature Infants Treated at Birth with a Single Dose of Synthetic Surfactant: A Multicenter Controlled Trial," *J. Pediatr.*, **118**, pp. 277-284.
- Jobe, A. H., 1993, "Pulmonary Surfactant Therapy," *N. Engl. J. Med.*, **328**, pp. 861-868.
- Yapicioglu, H., Yildizdas, D., Bayram, I., Sertdemir, Y., and Yilmaz, H. L., 2003, "The Use of Surfactant in Children with Acute Respiratory Distress Syndrome: Efficacy in Terms of Oxygenation, Ventilation and Mortality," *Pulm. Pharmacol. Ther.*, **16**, pp. 327-333.
- Salvia-Roiges, M. D., Carbonell-Estrany, X., Figueras-Aloy, J., and Rodriguez-Miguel, J. M., 2004, "Efficacy of Three Treatment Schedules in Severe Meconium Aspiration Syndrome," *Acta Paediatr.*, **93**, pp. 60-65.
- Hirschl, R. B., Croce, M., Gore, D., Wiedemann, H., Davis, K., Zwischenberger, J., and Bartlett, R. H., 2002, "Prospective, Randomized, Controlled Pilot Study of Partial Liquid Ventilation in Adult Acute Respiratory Distress Syndrome," *Am. J. Respir. Crit. Care Med.*, **165**, pp. 781-787.
- Shaffer, T. H., and Wolfson, M. R., 1996, "Liquid Ventilation: An Alternative Ventilation Strategy for Management of Neonatal Respiratory Distress," *Eur. J. Pediatr.*, **155**, Suppl 2, pp. S30-S34.
- Leach, C. L., Greenspan, J. S., Rubenstein, S. D., Shaffer, T. H., Wolfson, M. R., Jackson, J. C., DeLemos, R., and Fuhrman, B. P., 1996, "Partial Liquid Ventilation with Perflubron in Premature Infants with Severe Respiratory Distress Syndrome: The LiquiVent Study Group," *N. Engl. J. Med.*, **335**, pp. 761-767.
- Mikawa, K., Nishina, K., Takao, Y., and Obara, H., 2004, "Efficacy of Partial Liquid Ventilation in Improving Acute Lung Injury Induced by Intratracheal Acidified Infant Formula: Determination of Optimal Dose and Positive End-Expiratory Pressure Level," *Crit. Care Med.*, **32**, pp. 209-216.
- Cox, P. N., Frndova, H., Karlsson, O., Holowka, S., and Bryan, C. A., 2003, "Fluorocarbons Facilitate Lung Recruitment," *Intensive Care Med.*, **29**, pp. 2297-2302.
- Yu, J., and Chien, Y. W., 1997, "Pulmonary Drug Delivery: Physiologic and Mechanistic Aspects," *Crit. Rev. Ther. Drug Carrier Syst.*, **14**, pp. 395-453.
- Jensen, O. E., Halpern, D., and Grotberg, J. B., 1994, "Transport of a Passive Solute by Surfactant-Driven Flows," *Chem. Eng. Sci.*, **49**, pp. 1107-1117.
- Iqbal, S., Ritson, S., Prince, I., Denyer, J., and Everard, M. L., 2004, "Drug Delivery and Adherence in Young Children," *Pediatr. Pulmonol.*, **37**, pp. 311-317.
- Zhang, Y. L., Matar, O. K., and Craster, R. V., 2003, "A Theoretical Study of Chemical Delivery Within the Lung Using Exogenous Surfactant," *Med. Eng. Phys.*, **25**, pp. 115-132.
- Myrdal, P. B., Karlage, K. L., Stein, S. W., Brown, B. A., and Haynes, A., 2004, "Optimized Dose Delivery of the Peptide Cyclosporine Using Hydrofluoroalkane-Based Metered Dose Inhalers," *J. Pharm. Sci.*, **93**, pp. 1054-1061.
- Ueda, T., Ikegami, M., Rider, E. D., and Jobe, A. H., 1994, "Distribution of Surfactant and Ventilation in Surfactant-Treated Preterm Lambs," *J. Appl. Physiol.*, **76**, pp. 45-55.

- [17] Bull, J. L., Tredici, S., Komori, E., Brant, D. O., Grotberg, J. B., and Hirschl, R. B., 2004, "Distribution Dynamics of Perfluorocarbon Delivery to the Lungs: An Intact Rabbit Model," *J. Appl. Physiol.*, **96**, pp. 1633–1642.
- [18] Espinosa, F. F., and Kamm, R. D., 1998, "Meniscus Formation During Tracheal Instillation of Surfactant," *J. Appl. Physiol.*, **85**, pp. 266–272.
- [19] Cassidy, K. J., Bull, J. L., Glucksberg, M. R., Dawson, C. A., Haworth, S. T., Hirschl, R. B., Gavriely, N., and Grotberg, J. B., 2001, "A Rat Lung Model of Instilled Liquid Transport in the Pulmonary Airways," *J. Appl. Physiol.*, **90**, pp. 1955–1967.
- [20] Gilliard, N., Richman, P. M., Merritt, T. A., and Spragg, R. G., 1990, "Effect of Volume and Dose on the Pulmonary Distribution of Exogenous Surfactant Administered to Normal Rabbits or to Rabbits with Oleic Acid Lung Injury," *Am. Rev. Respir. Dis.*, **141**, pp. 743–747.
- [21] Anderson, J. C., Molthen, R. C., Dawson, C. A., Haworth, S. T., Bull, J. L., Glucksberg, M. R., and Grotberg, J. B., 2004, "Effect Of Ventilation Rate on Instilled Surfactant Distribution in the Pulmonary Airways of Rats," *J. Appl. Physiol.*, **97**, pp. 45–56.
- [22] Davis, J. M., Russ, G. A., Metlay, L., Dickerson, B., and Greenspan, B. S., 1992, "Short-Term Distribution Kinetics of Intratracheally Administered Exogenous Lung Surfactant," *Pediatr. Res.*, **31**, pp. 445–450.
- [23] Cassidy, K. J., Gavriely, N., and Grotberg, J. B., 2001, "Liquid Plug Flow in Straight and Bifurcating Tubes," *J. Biomech. Eng.*, **123**, pp. 580–589.
- [24] Weibel, E. R., 1963, "Morphometry of the Human Lung," Academic, New York.
- [25] Sauret, V., Halson, R. M., Brown, I. W., Fleming, J. S., and Bailey, A. G., 2002, "Study of the Three-Dimensional Geometry of the Central Conducting Airways in Man Using Computed Tomographic (CT) images," *J. Anat.*, **200**, pp. 123–134.
- [26] Fleming, J. S., Nassim, M., Hashish, A. H., Bailey, A. G., Conway, J., Holgate, S., Halson, P., Moore, E., and Martonen, T. B., 1995, "Description of Pulmonary Deposition of Radiolabeled Aerosol by Airway Generation Using a Conceptual 3-Dimensional Model of Lung Morphology," *Journal of Aerosol Medicine-Deposition Clearance and Effects in the Lung*, **8**(4), pp. 341–356.
- [27] Michael, D. H., 1981, "Meniscus Stability," *Annu. Rev. Fluid Mech.*, **13**, pp. 189–215.
- [28] Bogoy, D. B., 1979, "Drop Formation in a Circular Liquid Jet," *Annu. Rev. Fluid Mech.*, **11**, pp. 207–228.
- [29] Gauglitz, P. A., and Radke, C. J., 1990, "The Dynamics of Liquid Film Breakup in Constricted Cylindrical Capillaries," *J. Colloid Interface Sci.*, **134**, pp. 14–40.
- [30] Hammond, P. S., 1983, "Nonlinear Adjustment of a Thin Annular Film of Viscous Fluid Surrounding a Thread of Another Within a Circular Pipe," *J. Fluid Mech.*, **137**, pp. 363–384.
- [31] Kamm, R. D., and Schroter, R. C., 1989, "Is Airway Closure Caused by a Thin Liquid Instability?," *Respir. Physiol.*, **75**, pp. 141–156.
- [32] Cassidy, K. J., Halpern, D., Ressler, B. G., and Grotberg, J. B., 1999, "Surfactant Effects in Model Airway Closure Experiments," *J. Appl. Physiol.*, **87**, pp. 415–427.
- [33] Howell, P. D., Waters, S. L., and Grotberg, J. B., 2000, "The Propagation of a Liquid Bolus Along a Liquid-Lined Flexible Tube," *J. Fluid Mech.*, **406**, pp. 309–335.
- [34] Fujii, H., and Nakae, H., 1995, "Effect of Gravity on Contact-Angle," *Philos. Mag. A*, **72**, pp. 1505–1512.
- [35] Cassidy, K. J., 1999, "Liquid Film Dynamics in the Pulmonary Airways," Northwestern University, Evanston, IL, 171 pp.
- [36] Heistracher, T., and Hofmann, W., 1995, "Physiologically Realistic Models of Bronchial Airway Bifurcations," *J. Aerosol Sci.*, **26**, pp. 497–509.
- [37] Kim, H. Y., and Chun, J. H., 2001, "The Recoiling of Liquid Droplets Upon Collision with Solid Surfaces," *Phys. Fluids*, **13**, pp. 643–659.
- [38] Suresh, V., and Grotberg, J. B., 2005, "The Effect of Gravity On Liquid Plug Propagation in a Two-Dimensional Channel," *Phys. Fluids*, **17**(3), 031507.
- [39] Halpern, D., Jensen, O. E., and Grotberg, J. B., 1998, "A Theoretical Study of Surfactant and Liquid Delivery into the Lung," *J. Appl. Physiol.*, **85**, pp. 333–352.
- [40] Bracke, M., Devoeight, F., and Joos, P., 1989, "The Kinetics of Wetting—the Dynamic Contact-Angle," *Adv. Colloid Interface Sci.*, **79**, pp. 142–149.
- [41] Jiang, T. S., Oh, S. G., and Slattery, J. C., 1979, "Correlation for Dynamic Contact-Angle," *J. Colloid Interface Sci.*, **69**, pp. 74–77.
- [42] Hoffman, R. L., 1975, "Study of Advancing Interface. 1. Interface Shape in Liquid-Gas Systems," *J. Colloid Interface Sci.*, **50**, pp. 228–241.
- [43] Fujioka, H., and Grotberg, J. B., 2004, "Steady Propagation of a Liquid Plug in a 2-Dimensional Channel," *J. Biomech. Eng. Transaction of ASME*, **126**, pp. 567–577.